

Printed Circuit Heat Exchanger and Finned-Tube Heat Exchanger Modeling for a Supercritical CO₂ Power Cycle

Vamshi K. Avadhanula, Luke R. Magyar and Timothy J. Held
Echogen Power Systems (DE), Inc.
Akron, Ohio

ABSTRACT

This paper presents semi-empirical heat transfer and pressure-drop models of two large-scale Printed Circuit Heat Exchangers that were tested extensively on a 7.3MWe-scale sCO₂ power cycle. The models are discretized representations of the heat exchangers, which permit accommodation of the rapidly-varying thermodynamic and property variation of CO₂ over the pressure and temperature ranges encountered through the heat exchanger passages. Transient modeling of the heat exchangers also uses a discretized approach, including a discretized thermal mass model to predict the fluid outlet temperature evolution with time after rapid changes in inlet temperature, pressure and flow rate. For these cases, the inlet temperatures, pressures and flows are imposed based on measured values, and the outlet temperatures and pressures are modeled and compared to measurements.

This paper also presents semi-empirical heat transfer models of two finned-tube heat exchangers that can be used as primary heat exchangers (e.g., gas turbine exhaust heat recovery, and air-cooled coolers for heat rejection in sCO₂ applications). As no test data was available from testing of these heat exchangers in sCO₂ applications, they were modeled based on manufacturer-supplied design point data. Based on system transient modeling results, the characteristic response time of the finned-tube heat exchangers is more than an order of magnitude larger than that for PCHEs, thus limiting the overall system response rate.

INTRODUCTION

Supercritical carbon dioxide (sCO₂) power cycles are characterized by a high degree of recuperation, with the internally-recirculated heat frequently exceeding the rate of heat addition by a factor of three or more. The high conductance (UA) required for this large recuperation duty, accompanied by the high operating pressure of sCO₂ cycles requires the use of advanced, compact heat exchanger technology. The primary design used to date is the so-called "Printed Circuit Heat Exchanger" (PCHE), which consists of layers of chemically etched metal plates in a diffusion-bonded assembly [1]. These heat exchangers have proven to be robust in gas cooling service, with many years of successful field experience. While PCHEs have been proposed as the heat exchanger technology of choice for commercial-scale sCO₂ power cycles [2,3], practical experience for power-cycle applications has been limited to laboratory-scale systems [4–6] until recently, when a commercial-scale (7.3MWe) sCO₂ system, termed the EPS100, underwent an extensive factory test campaign [7].

Heat exchanger performance can be quantified in numerous ways. Heat transfer performance can be evaluated by conductance ($UA=Q/\Delta T_m$, where Q is the total transferred heat, and ΔT_m is an appropriately-defined mean temperature difference between the two fluid streams). The pressure drop across each side

of the heat exchanger has an influence on both the heat transfer performance and overall cycle performance. Finally, heat exchanger life is critical to the successful deployment of sCO₂ power cycles. Heat exchanger life can be divided into performance degradation (e.g. fouling) and thermo-mechanical factors. Given that PCHEs are designed to ASME Boiler and Pressure Vessel code requirements, steady-state hydraulic and thermal stress are unlikely to be life-limiting. Thermomechanical life is more likely to be limited by severe thermal transients that could be generated during extreme incidents [8,9], such as emergency stops or turbine trips.

To properly evaluate the transient thermal stresses that PCHEs will be expected to withstand, it is first necessary to establish realistic transient boundary conditions that will be encountered in service. The present paper represents part of a larger study to define and validate a large-scale transient model of the EPS100 [10]. The full system model is still under development, and is not yet capable of simulating the entire operational envelope. Thus, for the present work, the sub-system model of the heat exchangers is used with imposed boundary conditions (inlet flows, temperatures and pressures) from the measured test data. This data set covers a broad range of operating conditions, which encompass system initial start, turbocompressor “bootstrapping,” power turbine start, quasi-steady-state operation, and system trips. The transient performance of the heat exchanger model is compared to the measured responses of the two PCHEs in the EPS100 for model validation purposes. It is the intent of this study to establish the framework for full system simulations of both normal and extreme upset transient conditions, which can then be used to determine the expected cyclic life of the PCHEs.

In certain sCO₂ power cycle applications, finned-tube heat exchangers are used for exhaust gas-to-CO₂ (heat source) and CO₂-to-air (heat sink) heat transfer. The thermal mass (physical mass multiplied by heat capacity) of finned-tube heat exchangers is an order of magnitude larger than PCHE thermal mass for the same conductance (UA) due to the low heat transfer coefficient on the exhaust / air side of the heat exchanger.

The ratio of thermal mass to conductance approximately defines the characteristic response time of a heat exchanger by writing a simplistic first order equation for the rate of change of bulk heat exchanger temperature

$$mc \frac{dT}{dt} = UA (\Delta T_m - \Delta T_{m,ss}),$$

where $\Delta T_{m,ss}$ is the steady-state value of mean temperature difference between the fluid streams. Assuming the temperature terms are of similar order of magnitude, a characteristic time scale can be defined as:

$$\tau = \frac{mc}{UA}$$

The physical mass, UA and characteristic time values for the four heat exchangers analyzed in this study are listed in Table 1. The characteristic time scale of finned-tube heat exchangers will, in general, control the time scale for the sCO₂ power cycle to reach steady state for any sudden changes in the boundary conditions (flow or inlet temperatures) and ultimately define the sCO₂ cycle control system time constants.

MODELING PLATFORM

The transient simulations are conducted using the GT-SUITE [11] system simulation software platform. GT-SUITE is a 1D engineering system simulation software, and includes tools for analyzing mechanical, flow, thermal, electromagnetic and control systems. GT-SUITE solves 1D Navier-Stokes equations along flow components, and solution convergence is checked using pressure, continuity and energy residuals. Component models can be built based on GT-SUITE supplied and/or user-defined component templates. Component templates can utilize manufacturer data and/or test data to calibrate the component. Individual components, such as heat exchangers, pumps, turbines, can then be simulated and validated using subsystem boundary conditions. GT-SUITE uses NIST REFPROP [12] for calculating fluid thermal and transport properties. Further details of the modeling process and assumptions used in the overall system modeling can be found in Reference [10].

SYSTEM CONFIGURATION

The EPS100 is a 7.3MWe net power $s\text{CO}_2$ power cycle designed for commercial operation, utilizing the exhaust heat of a 20-25MWe gas turbine as the heat source. The details of the production cycle configuration and of an uprated version capable of over 9MWe from the same heat source, are described in Reference [3], and a simplified PFD in the as-tested configuration is shown in Figure 1. The EPS100 uses a constant-speed “power” turbine (T-2) connected to a gearbox-driven synchronous generator for power generation, and a separate, variable-speed turbocompressor (CP-1 and T-1) to provide high-pressure CO_2 to operate the cycle. In the as-tested configuration [7], the primary heat exchanger (RC-1) transfers heat from an external source (in the factory test case modeled here, steam from facility boilers) to the working fluid, which then drives the two turbines in parallel. A single PCHE recuperator (RC-2) recovers residual enthalpy from the turbine exhausts by preheating the working fluid, and the remainder of the excess enthalpy is transferred to cooling tower water in the heat rejection heat exchanger (HRHX) (CX-1), another PCHE.

HEAT EXCHANGER MODELS

Printed Circuit Heat Exchanger Models

In the present study, the recuperator and HRHX are simulated using the built-in plate heat exchanger (PHE) models in GT-SUITE. From a heat transfer and pressure loss perspective, PCHEs and PHEs have similar governing equations, as both are primarily counter-flow geometry, and the fluid flow is well within the turbulent regime. Thus, classical Nusselt number and friction factor functional forms of the heat transfer and pressure loss coefficients can be applied. The PCHE is simulated by applying a heat transfer area multiplier to account for the smaller passage dimensions relative to a conventional PHE. The heat transfer process is discretized into 25 sub-volumes to account for the variation in fluid properties as the temperature and pressure vary across the length of the heat exchanger. The thermal mass of the heat exchanger is set equal to the physical mass of the actual heat exchanger multiplied by the temperature-dependent heat capacity of the 316L stainless steel material. The heat transfer process is modeled as a series of thermal resistances. The baseline heat transfer coefficients are modeled after classical heat transfer correlations with variable coefficients, with a simple one-dimensional thermal conduction resistance between the two fluids.

Figure 4 shows the recuperator model in isolation. Within the recuperator, relatively low-pressure, high-temperature CO_2 from the turbine exhaust transfers heat to the high-pressure, low-temperature CO_2 from

the compressor discharge. The recuperator heat transfer coefficients are based on single-phase Dittus-Boelter correlations on both fluid sides, with coefficients calibrated using a subset of steady-state data points taken from test data. The calibration process utilizes measured fluid flow rates, inlet temperatures, inlet and outlet pressures, and overall heat transfer rate. Using this information, the software adjusts the heat transfer and pressure drop coefficients to best match the supplied data.

The PCHE water-cooled heat rejection heat exchanger model is constructed and validated in a similar manner as the recuperator. In the HRHX, CO₂ from the recuperator exhaust transfers heat to water from a cooling tower. As the EPS100 operates in both supercritical and transcritical (condensing) mode, the HRHX is modeled as a two-phase heat exchanger on the CO₂ side. For single-phase heat transfer, Dittus-Boelter correlations are used, while the correlation of Yan et al. [13] was used for condensation heat transfer. For single-phase conditions, standard friction factor correlations were used, and for two-phase Friedel [14] correlations were used to model pressure loss coefficients on CO₂ side.

The heat exchanger calibration process was validated by using simulating several steady-state operating points for the two heat exchangers. The modeled outlet conditions are shown in Figures 2 and 3 as a function of the measured outlet conditions. The agreement is excellent, with calculated weighted regression errors of 0.56% and 0.91% for overall heat transfer rate for the recuperator and HRHX respectively.

Finned-Tube Heat Exchanger Models

For the finned-tube primary heat exchanger (PHX) and air-cooled cooler (ACC), GT-SUITE built-in finned-tube heat exchanger model templates were used for simulations. For the calibration of finned-tube heat exchangers, the manufacturer-provided design point data was used. Note that the manufacturer quotations obtained for PHX and ACC were based on a sCO₂ power block similar to EPS100 system described above. Physical geometry information from the quotations were directly used in the model without the need for heat transfer area multipliers (unlike PCHE above). Like the PCHE model, the heat transfer process is discretized into 25 sub-volumes to account for the variation in fluid properties as the temperature and pressure vary across the tube length of the heat exchanger. The thermal mass of the heat exchangers is again set equal to the physical mass of the actual heat exchanger multiplied by the temperature-dependent heat capacity of the 316L stainless steel material.

In a typical field installation of sCO₂ power cycle for gas turbine exhaust heat recovery, within the primary heat exchanger, exhaust gases on the fin side transfer heat to high-pressure CO₂ (usually from recuperator) on the tube side. The PHX is a single tube-bundle heat exchanger unit, i.e. no bays as ACC. The PHX was modeled as single-phase heat transfer with CO₂ on tube side and gas turbine exhaust on fin side fluids. Thermophysical properties of air were assumed in place of exhaust. A Dittus-Boelter correlation was used for the tube side and a Colburn correlation for fin-side heat transfer coefficients. Standard friction factor correlations were used to model pressure loss coefficients on both tube and fin sides.

Figure 5 shows the model of a single bay of the ACC with three fans. CO₂ on the tube side (usually from the low pressure recuperator exhaust) transfers heat to the cross-flowing cooling air from ACC fans on the fin side. For a EPS100 system described above, to handle the cooling loads of the cycle we will need seven bays in parallel with 21 fans (Figure 6). The CO₂ flow from the recuperator exhaust is distributed almost uniformly among seven bays and the cooled (or condensed) CO₂ from each bay is converged into

single header before returning to the compressor inlet. Modeling of the ACC involves two components, heat exchanger model (tube bundle) as well as fan model using fan curves from manufacturer. The ACC was modeled as two-phase heat transfer on tube side and single-phase on fin side as it is designed to operate in both supercritical and transcritical (condensing) mode. For single-phase heat transfer, Dittus-Boelter correlations are used, while the correlation of Dobson and Chato [15] was used for condensation heat transfer. For single phase standard friction factor correlations and for two-phase Friedel [14] correlations were used to model pressure loss coefficients in tubes on CO₂ side.

As the PHX and ACC were modeled based on standard heat transfer correlations (without test data calibration), the models were validated using the manufacturer-predicted performance over different inlet boundary conditions as shown in Figures 7 and 8 respectively.

HEAT EXCHANGER SIMULATION RESULTS

Printed Circuit Heat Exchanger Simulation Results

The transient simulations are based on data collected during an extensive series of factory tests on the EPS100 system to evaluate operation, controls and performance [4]. Each day, the test system was run from a cold start to full load operation, with the goal of maximizing the power turbine output. For these simulations, the boundary condition values (heat exchanger inlet temperatures and flows) are taken from the test data, and input to the model, thus allowing the heat exchangers to be effectively modeled in isolation.

The overall comparison of the heat transfer rates and pressure drops across the recuperator and HRHX are shown in Figures 9-13. At the initial stage of the test, CO₂ is being circulated at a low rate through the system by a small motor-driven compressor, and heated by the primary heat exchanger. This flow causes the compressor drive turbine (T-1) to rotate at a relatively low speed, and the main compressor (CP-1) flow is diverted to the HRHX inlet through a bypass valve. Once the system is in an appropriate state (1555 seconds in Figures 15 and 16), the system operator commands the turbocompressor to transition to self-sustaining operation, termed “bootstrap,” and the main compressor flow supplies the drive turbine, which in turn causes it to accelerate to its nominal speed. This bootstrapping operation causes a step change in system flow as shown in Figure 16. Next, the power turbine (T-2), which was initially bypassed and isolated from the CO₂ flow rate, is accelerated to synchronous speed (“power turbine start”, 3986-4611 seconds), and then progressively loaded by connecting variable resistive load banks to the generator. The test was terminated by an indicated fault in one of the load banks at 31917 seconds, which resulted in a commanded system trip.

For the most part, the comparison is favorable, as would be expected following the calibration process as described previously. The time scale in the Figures 9-13 is too long to discern transient heat transfer effects, which are evaluated below.

One area of interest in the quasi-steady-state comparison and the ability of the model to capture the heat transfer and pressure drop phenomenon is the HRHX transition through the supercritical pressure at inlet to subcritical pressures at outlet on CO₂-side (Figure 14). In Figure 14, from around 9300 seconds to 13600 seconds, HRHX CO₂ inlet pressure is supercritical and outlet pressure is subcritical. As part of the test system control strategy, the “low-side” pressure is actively controlled as a function of the measured compressor inlet temperature. Initially, the cooling tower water is relatively cold, both due to the thermal inertia of the water contained within the tower basin, and to the lower wet-bulb temperature in the early

part of the day. As the test (and day) progressed, the cooling tower water temperature increased. The control system then increased the compressor inlet pressure in response to the higher measured CO₂ temperature at the compressor inlet. This caused the compressor inlet pressure to transition from subcritical to supercritical values at around 13600 seconds. Before this time duration, the CO₂ flow within the HRHX is in the two-phase condensing regime—the numerical code automatically switches between single-phase and two-phase correlations.

To evaluate the model's capability of simulating the transient response of the recuperator and HRHX, the rapid thermal transients that occurred during the bootstrap process were examined in more detail. During steady-state operation, the amount of heat transferred from the hot fluid would be expected to be equal the amount transferred to the cold fluid (with a small deviation due to external heat losses from the heat exchanger exterior surface to the environment). However, under transient heating conditions such as encountered during the bootstrap process, we expect that the thermal inertia of the heat exchanger should result in time delays between the hot-side heat transfer rate, and the cold-side heat transfer rate. But due to the highly compact nature and counterflow arrangement within PCHE, the thermal lag between the hot fluid and cold fluid response times were unnoticeable or very minute. This nature of PCHEs was validated both by test data and simulations as shown in Figures 15 to 17.

In Figure 16, it can be noticed that the water side and CO₂ side heat transfer rate in HRHX had about 22 seconds to 25 seconds time delay. The water discharge temperature measurement location was approximately 20 meters downstream of the HRHX, resulting in a convective lag that was modeled by adding an appropriate pipe length to the model.

Finned-Tube Heat Exchanger Simulation Results

In a typical sCO₂ exhaust heat recovery application, finned-tube heat exchangers will be used for the PHX and ACC. Because of their long time constants and large internal fluid volumes, accurate transient simulations of these heat exchangers are vital to developing optimal power cycle controls.

In gas turbine exhaust heat recovery service, the PHX can experience step changes in exhaust flow or temperature or both depending on the load demand on the turbine. On the other hand, for an ACC a step change in ambient temperature and air flow (for a constant speed fan) may not be a realistic assumption, but the CO₂ side can experience step changes in inlet flow or temperature or both, due to rapid transient behavior of the sCO₂ cycle. Figures 18 to 21 shows the transient response simulation results of PHX and ACC for a step change in flow or inlet temperature on one fluid side. For the simulations of Figures 18 to 21, only one inlet boundary condition parameter on a fluid side is changed while keeping the other inlet parameters constant, for example in Figure 18 only exhaust temperature has step change from 430°C to 485°C while keeping the exhaust flow rate, CO₂ flow rate and CO₂ inlet temperature constant.

From Figures 18 and 19, the PHX takes about 1500 seconds to reach steady-state operation for a step change in exhaust temperature and about 2000 seconds for a step change in exhaust flow rate. In comparison, the ACC takes about 600 seconds to reach steady state for a step change in CO₂ flow (Figure 20) and 200 seconds for a step change in CO₂ inlet temperature (Figure 21). The corresponding "1/e" time scales for the PHX are approximately 160-235 seconds, and 50-100 seconds for the ACC, comparable to those estimated in Table 1. The shorter time for the ACC to reach steady state compared to the PHX can be explained by the characteristic time (τ) scale shown in Table 1 as for ACC τ is more than half the PHX.

One important observation regarding thermal response time on CO₂ side in PHX simulations (Figures 18 and 19) is that the increase in CO₂ heat transfer rate (which implies CO₂ outlet temperature rise) occurs almost immediately for any changes in exhaust conditions (either flow or temperature). Engineering intuition might lead one to expect a large a thermal lag on CO₂ heat transfer rate (or outlet temperature) due to the PHX thermal mass (or physical mass: Table 1). However, the general counterflow arrangement of the exhaust flow relative to the CO₂ flowing in the tube bundle is such that the row of tubes exiting the PHX is immediately affected by a change in exhaust inlet conditions, and is not buffered by the thermal mass of the PHX.

CONCLUSION

Transient modeling of the recuperator and HRHX heat exchangers from a 7.3MWe sCO₂ power cycle test bench has been conducted. GT-SUITE system simulation code was used for this study. The quasi-steady-state as well as transient heat transfer behavior of the heat exchangers, and the single-phase and two-phase pressure drop behavior, can be modeled with reasonable accuracy. The simulation results for the recuperator and HRHX were in good agreement with the measured test data.

Due to highly compact nature of PCHes, the transient response time for a fluid is very short for any changes in inlet conditions on other fluid side, while the finned-tube heat exchangers have a transient response time approximately two orders of magnitude longer. Therefore, in an sCO₂ power cycle field installation, the finned-tube heat exchangers will define the system time constants, which will also define the plant control system requirements.

REFERENCES

- [1] Le Pierres, R., Southall, D., and Osborne, S., 2011, "Impact of Mechanical Design Issues on Printed Circuit Heat Exchangers," *Proceedings of sCO₂ Power Cycle Symposium*, Boulder, Colorado.
- [2] Dostal, V., Driscoll, M. J., and Hejzlar, P., 2004, *A Supercritical Carbon Dioxide Cycle for next Generation Nuclear Reactors*, Technical Report MIT-ANP-TR-100, Massachusetts Institute of Technology.
- [3] Held, T. J., 2015, "Supercritical CO₂ Cycles for Gas Turbine Combined Cycle Power Plants," *Power Gen International*, Las Vegas, Nevada.
- [4] Wright, S. A., Radel, R. F., Vernon, M. E., Rochau, G. E., and Pickard, P. S., 2010, *Operation and Analysis of a Supercritical CO₂ Brayton Cycle*, SAND2010-0171.
- [5] Kimball, K. J., and Clementoni, E. M., 2014, "Supercritical Carbon Dioxide Brayton Power Cycle Development Overview," *The 4th International Symposium – Supercritical CO₂ Power Cycles*, Pittsburgh, Pennsylvania.
- [6] Cho, J., Shin, H., Ra, H.-S., Lee, G., Roh, C., Lee, B., and Baik, Y.-J., 2016, "Development of the Supercritical Carbon Dioxide Power Cycle Experimental Loop in KIER," GT2016-57460, *ASME Turbo Expo 2016: Turbomachinery Technical Conference and Exposition*.
- [7] Held, T. J., 2014, "Initial Test Results of a Megawatt-Class Supercritical CO₂ Heat Engine," 4th Int. Symp. - Supercrit. CO₂ Power Cycles.
- [8] Gezelius, K., 2004, "Design of Compact Intermediate Heat Exchangers for Gas Cooled Fast Reactors," Massachusetts Institute of Technology.

- [9] Pra, F., Tochon, P., Mauget, C., Fokkens, J., and Willemsen, S., 2008, "Promising Designs of Compact Heat Exchangers for Modular HTRs Using the Brayton Cycle," *Nucl. Eng. Des.*, **238**(11), pp. 3160–3173.
- [10] Avadhanula, V. K., and Held, T. J., 2017, "Transient Modeling of a Supercritical CO₂ Power Cycle and Comparison with Test Data," GT2017-63279, *ASME Turbo Expo 2017: Turbomachinery Technical Conference and Exposition*, Charlotte, NC.
- [11] Anonymous, 2016, "GT-SUITE Overview" [Online]. Available: <https://www.gtisoft.com/gt-suite/gt-suite-overview/>. [Accessed: 21-Nov-2016].
- [12] Lemmon, E. W., Huber, M. L., and McLinden, M. O., 2013, "NIST Standard Reference Database 23: Reference Fluid Thermodynamic and Transport properties—REFPROP."
- [13] Yan, Y.-Y., Lio, H.-C., and Lin, T.-F., 1999, "Condensation Heat Transfer and Pressure Drop of Refrigerant R-134a in a Plate Heat Exchanger," *Int. J. Heat Mass Transf.*, **42**(6), pp. 993–1006.
- [14] Friedel L., 1987, "Improved friction pressure drop correlation for horizontal and vertical two-phase pipe flow," European Two-Phase Flow Group Meeting, Ispra, Paper 2.
- [15] Dobson, M. K., and Chato, J. C., 1998, "Condensation in Smooth Horizontal Tubes," *J. Heat Transfer*, **120**(1), pp. 193– 213.

Table 1: Physical mass of different heat exchangers considered in present study

	HRHX (PCHE)	Recuperator (PCHE)	PHX (Finned-tube HE)	ACC (Finned-tube HE)
Mass (kg)	14890	3470	54431	46274 (One Bay)
UA (kW/K)	4811	201	196	402
τ (seconds)	1.5	9	139	60

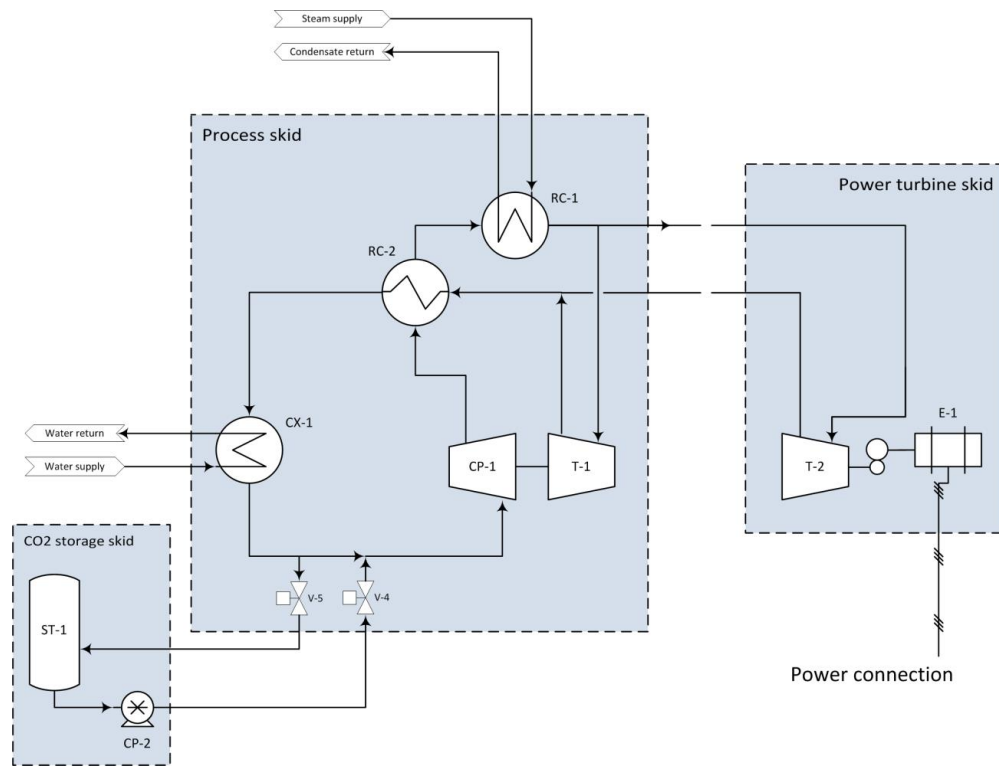


Figure 1: EPS100 test installation process flow diagram (PFD)

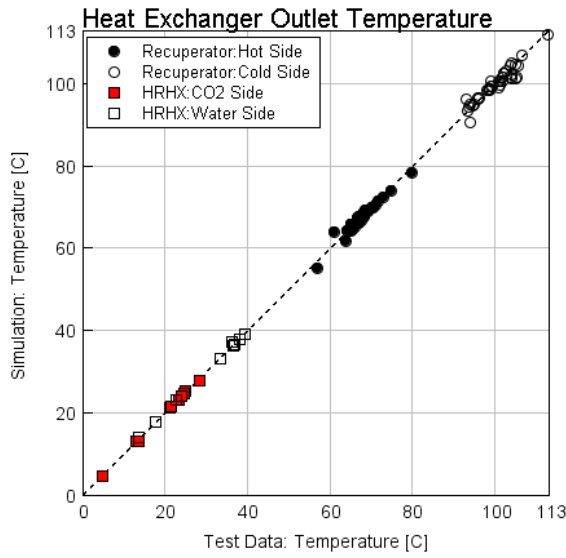


Figure 2: Recuperator and HRHX outlet temperatures from validation simulation

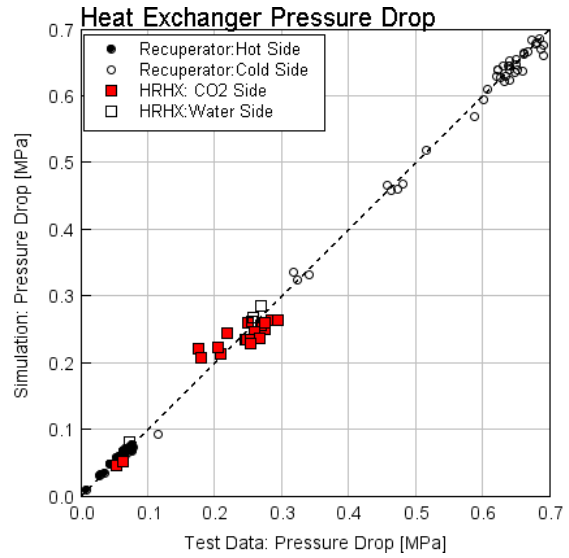


Figure 3: Recuperator and HRHX pressure drops from validation simulation

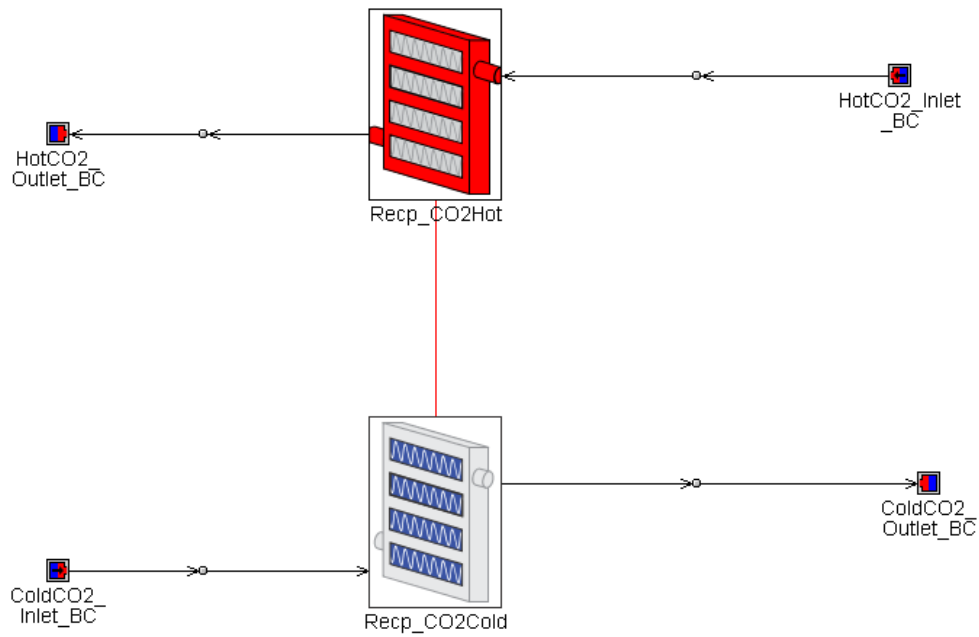


Figure 4: Recuperator model with boundary conditions

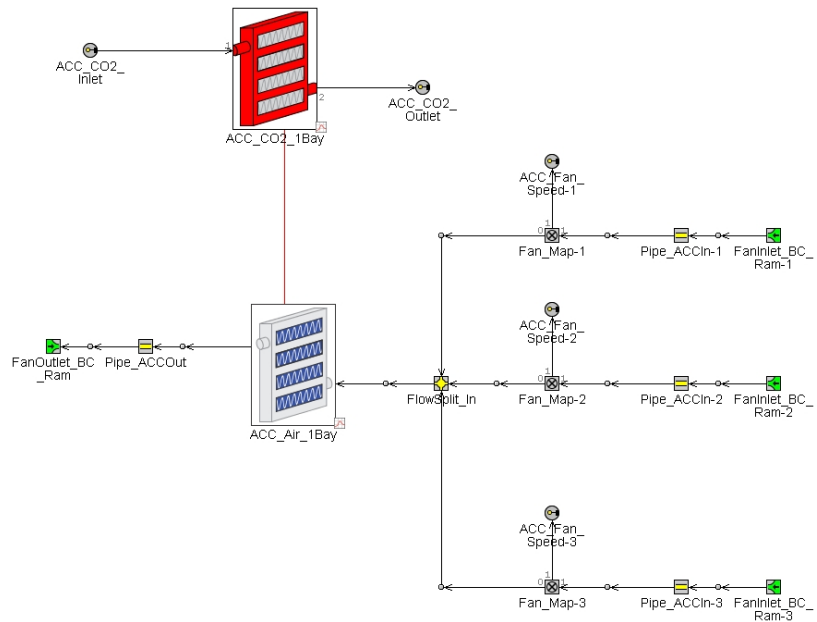


Figure 5: ACC single bay with three fans model

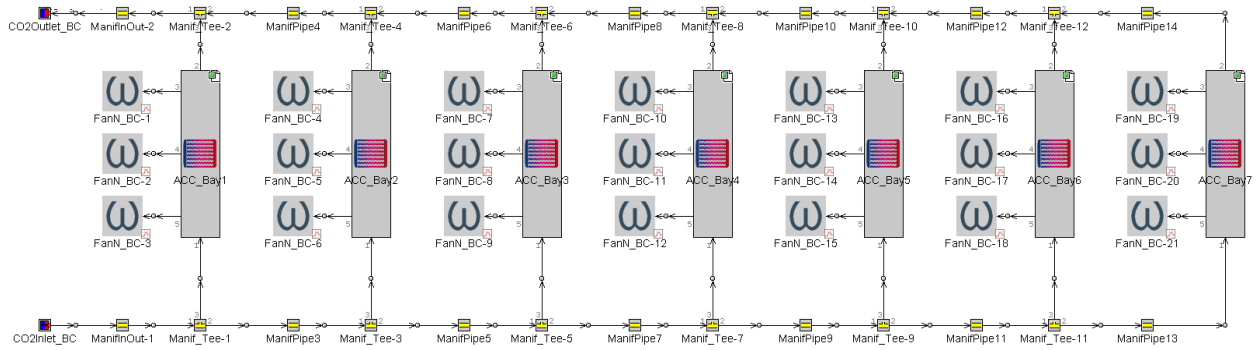


Figure 6: ACC seven bays model with twenty-one fans

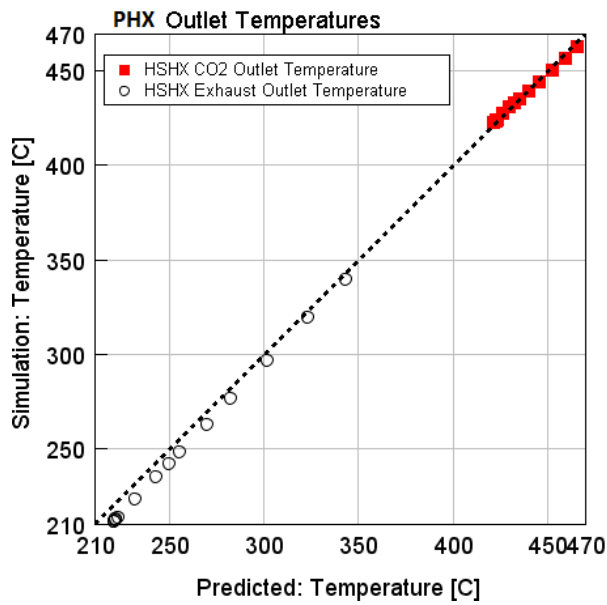


Figure 7: PHX CO₂ and exhaust outlet temperatures from validation

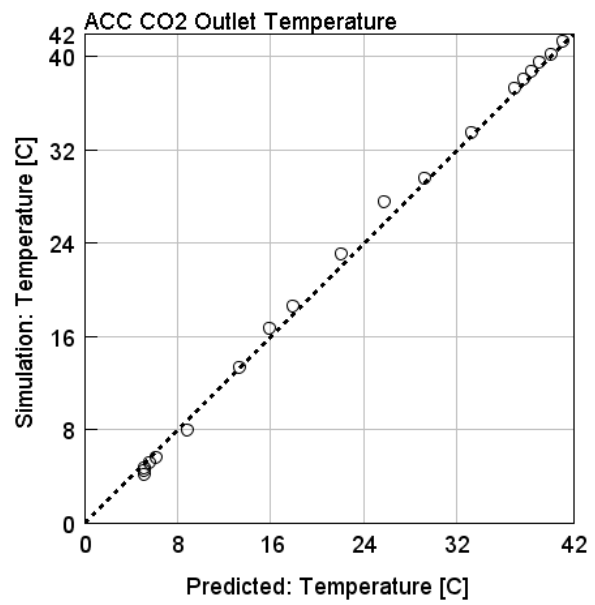


Figure 8: ACC CO₂ outlet temperatures from validation (seven bays simulation)

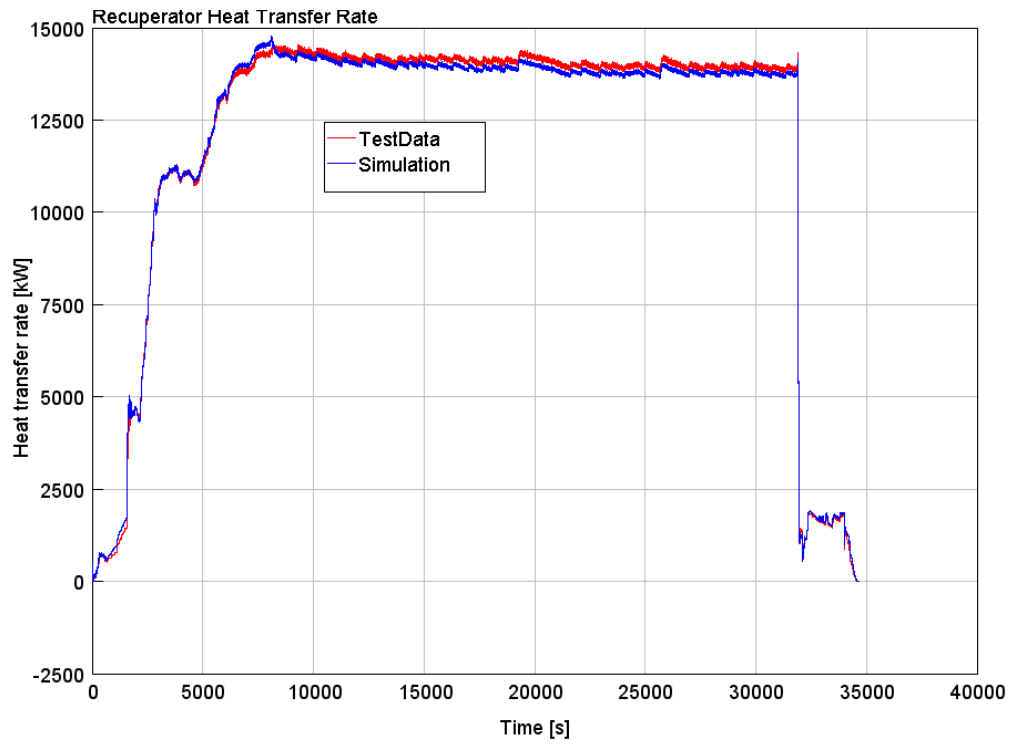


Figure 9: Recuperator heat transfer rate

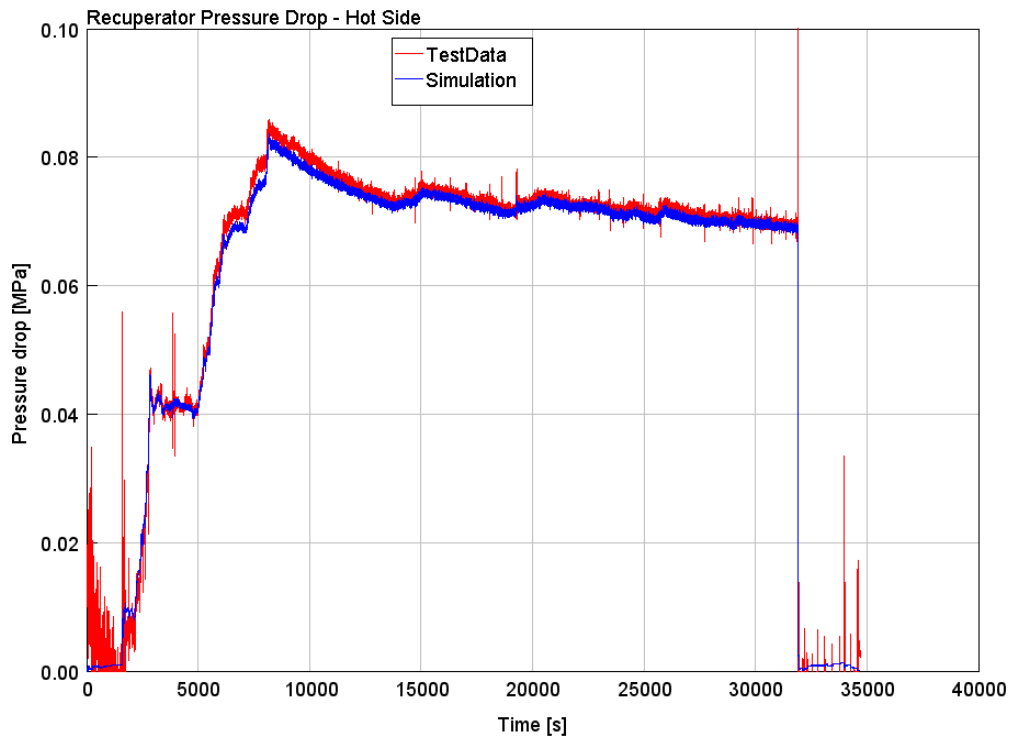


Figure 10: Recuperator low-pressure side pressure drop

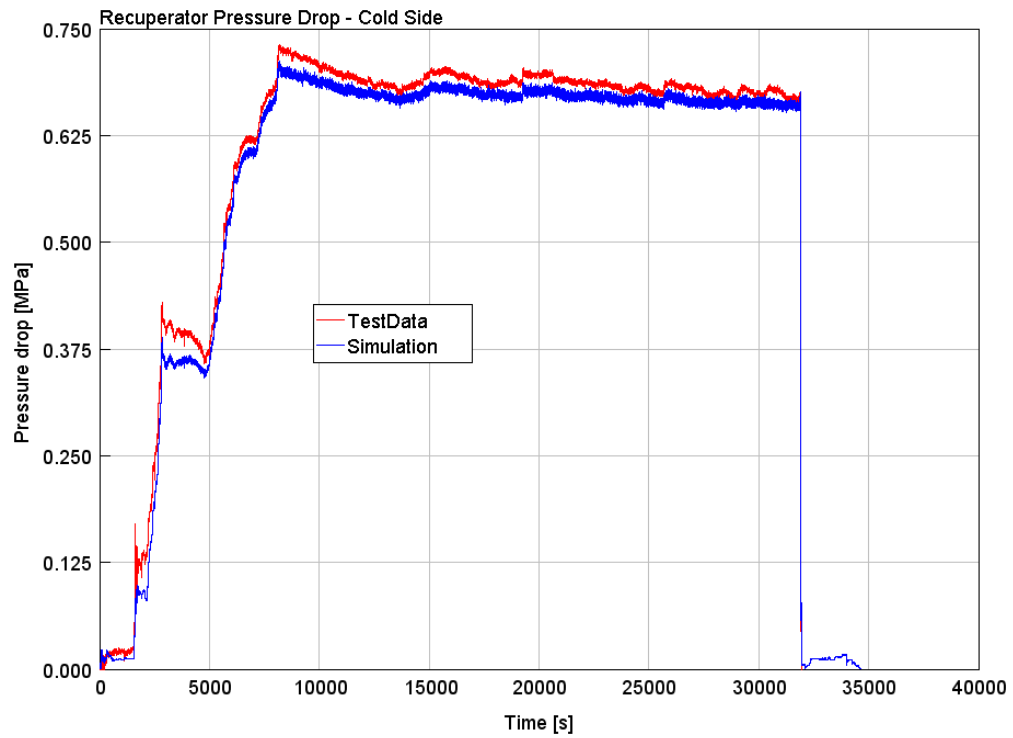


Figure 11: Recuperator high-pressure side pressure drop

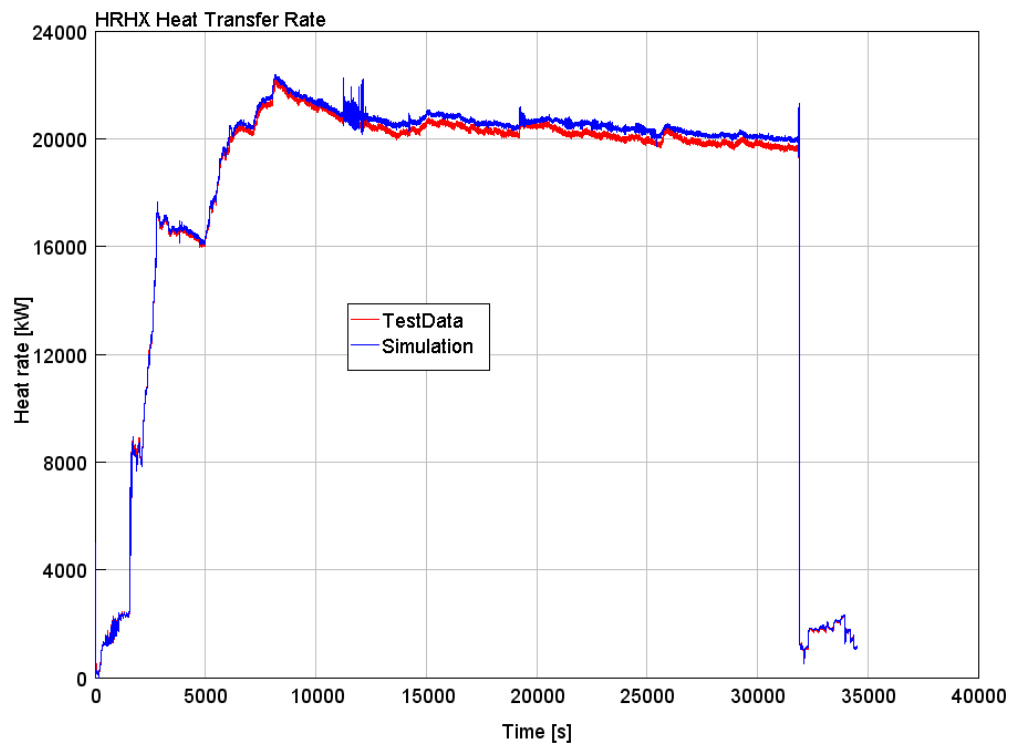


Figure 12: HRHX heat transfer rate

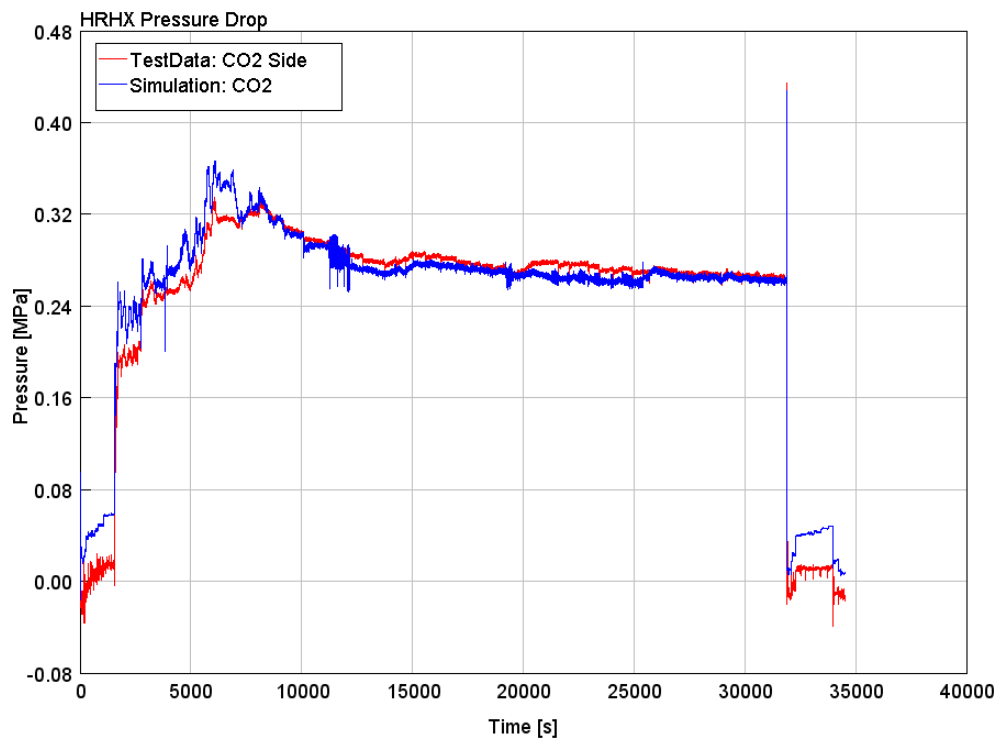


Figure 13: HRHX pressure drop on CO₂ side

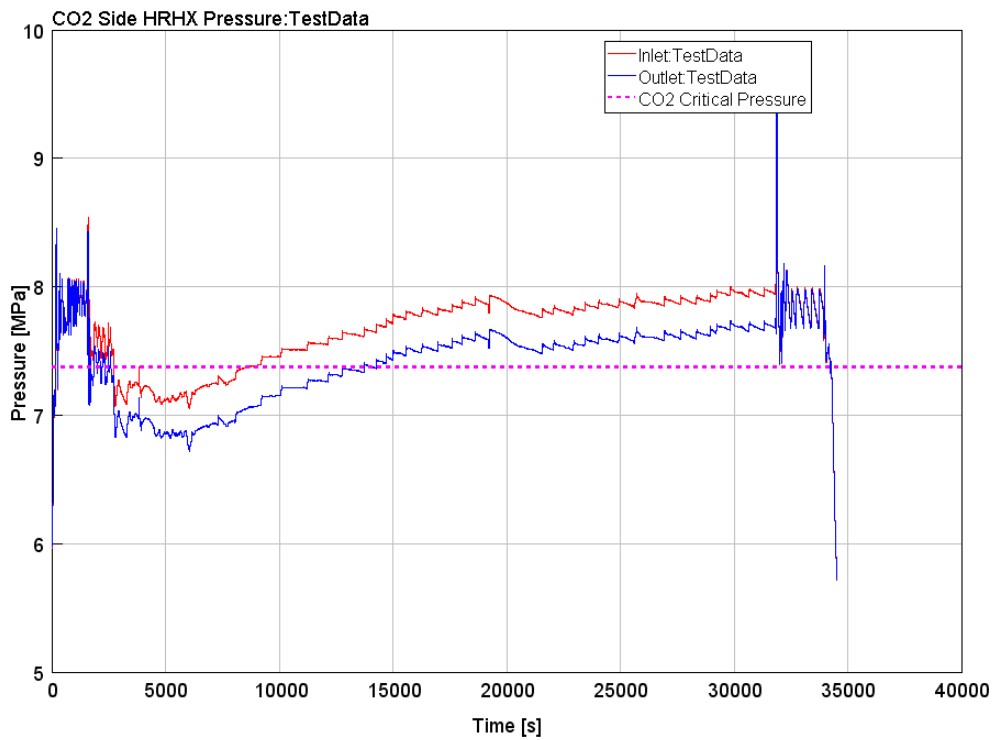


Figure 14: HRHX measured inlet and outlet pressures

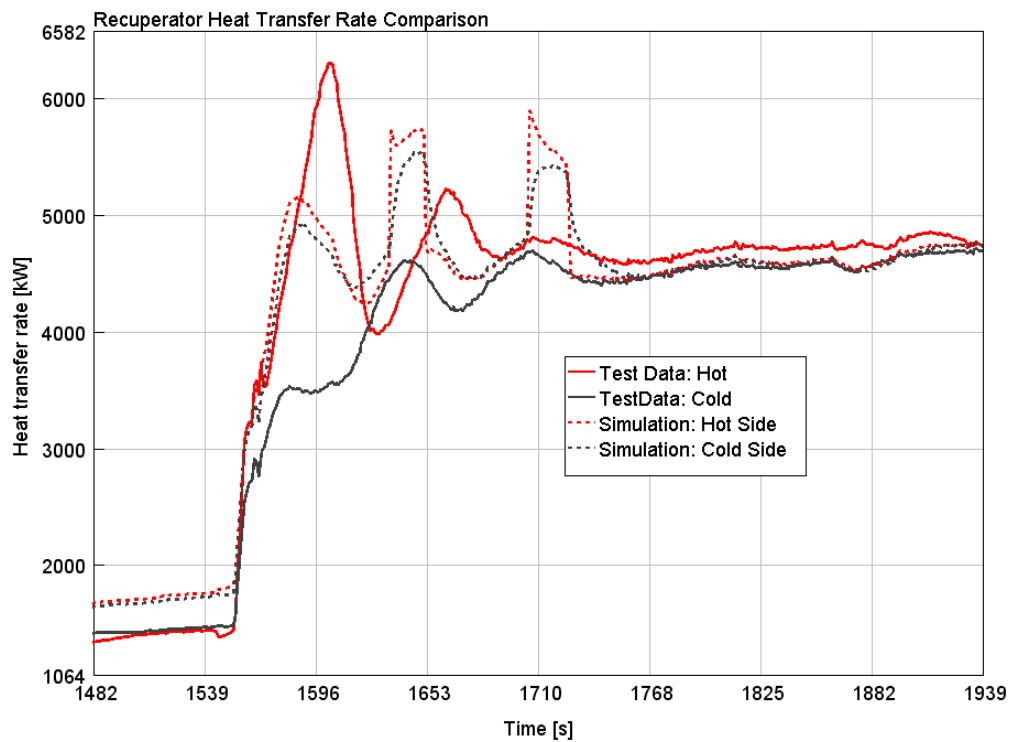


Figure 15: Measured thermal response of recuperator during rapid transient

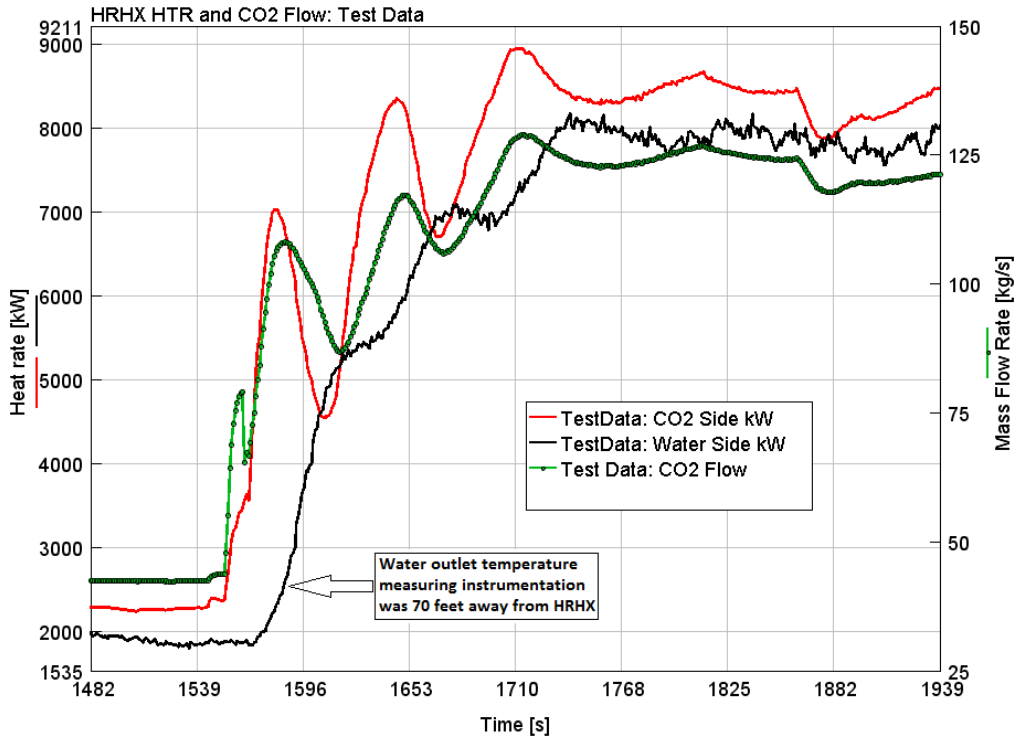


Figure 16: Measured thermal response of HRHX during rapid transient

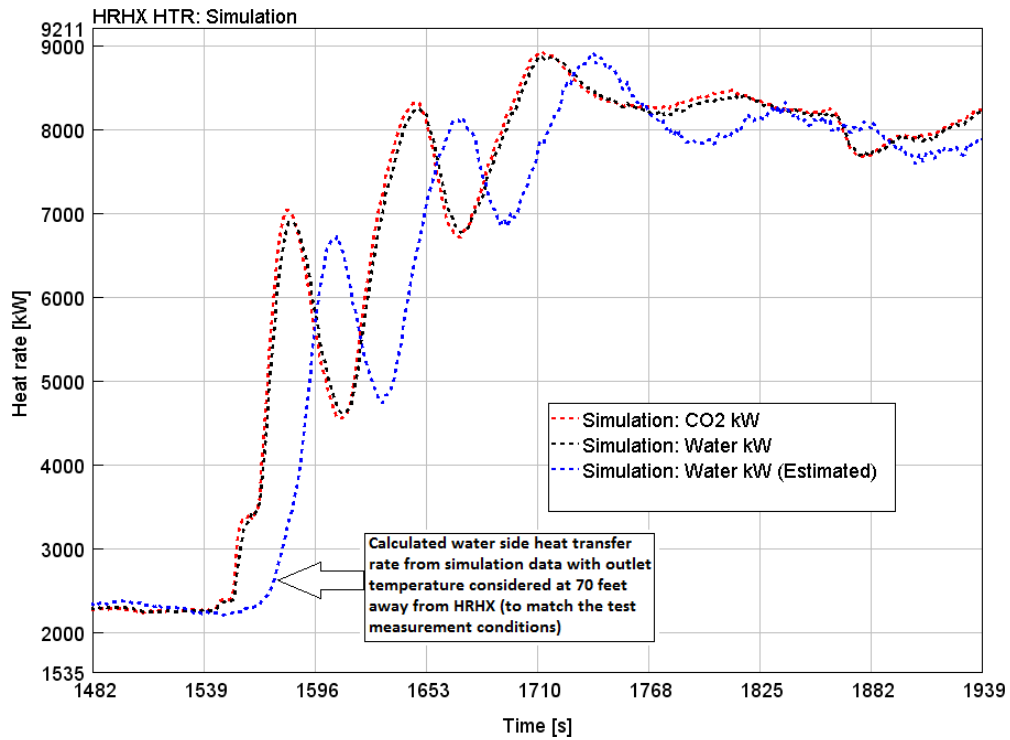


Figure 17: Modeled thermal response of HRHX during rapid transient

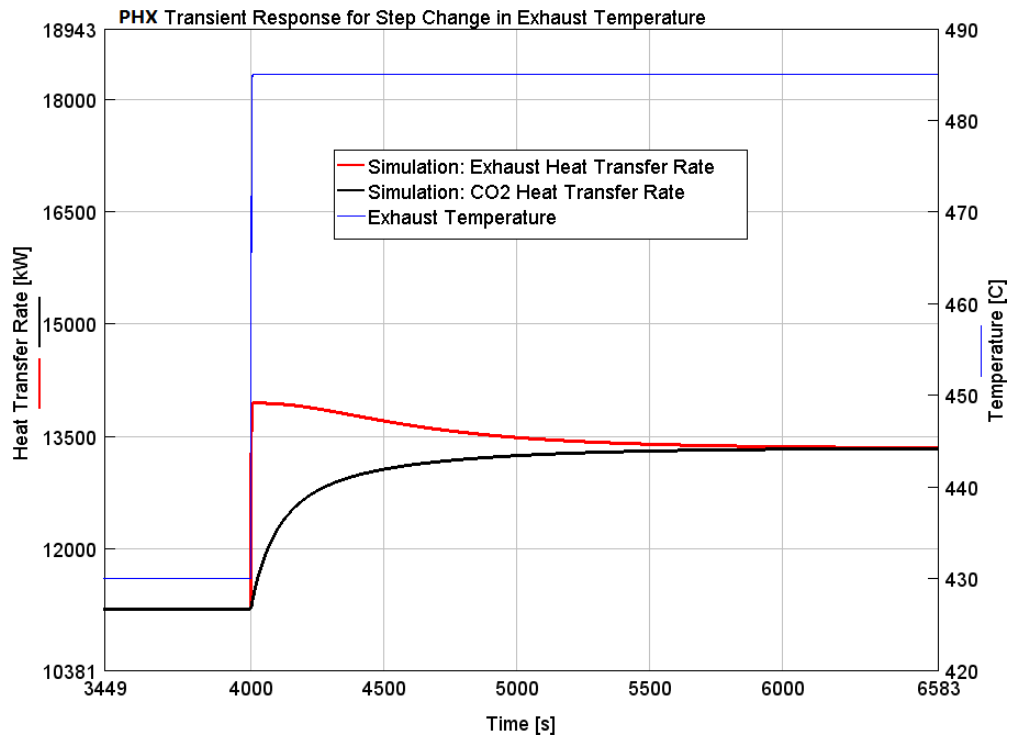


Figure 18: PHX transient response for a step change in gas turbine exhaust temperature

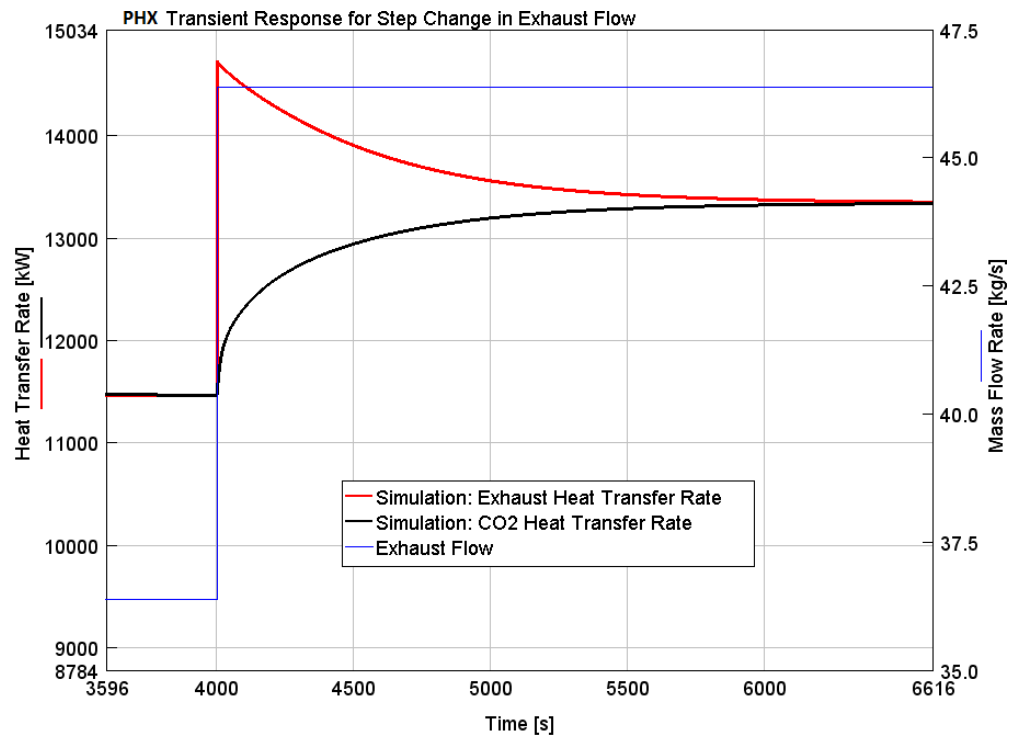


Figure 19: PHX transient response for a step change in gas turbine exhaust flow rate

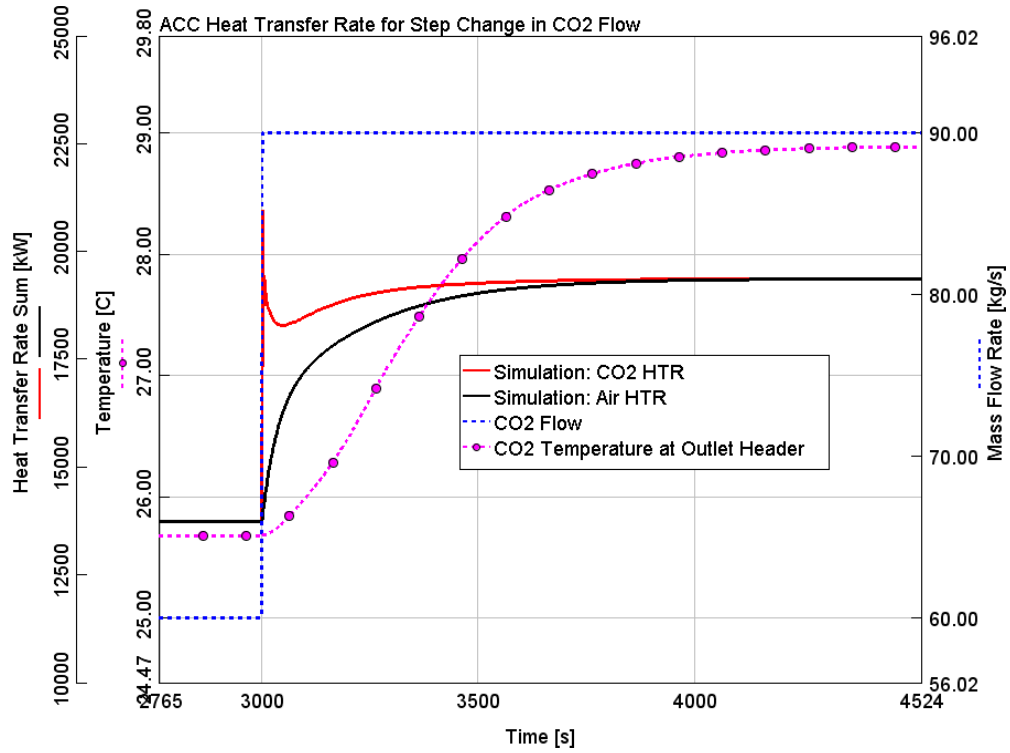


Figure 20: ACC transient response for a step change in CO₂ flow rate

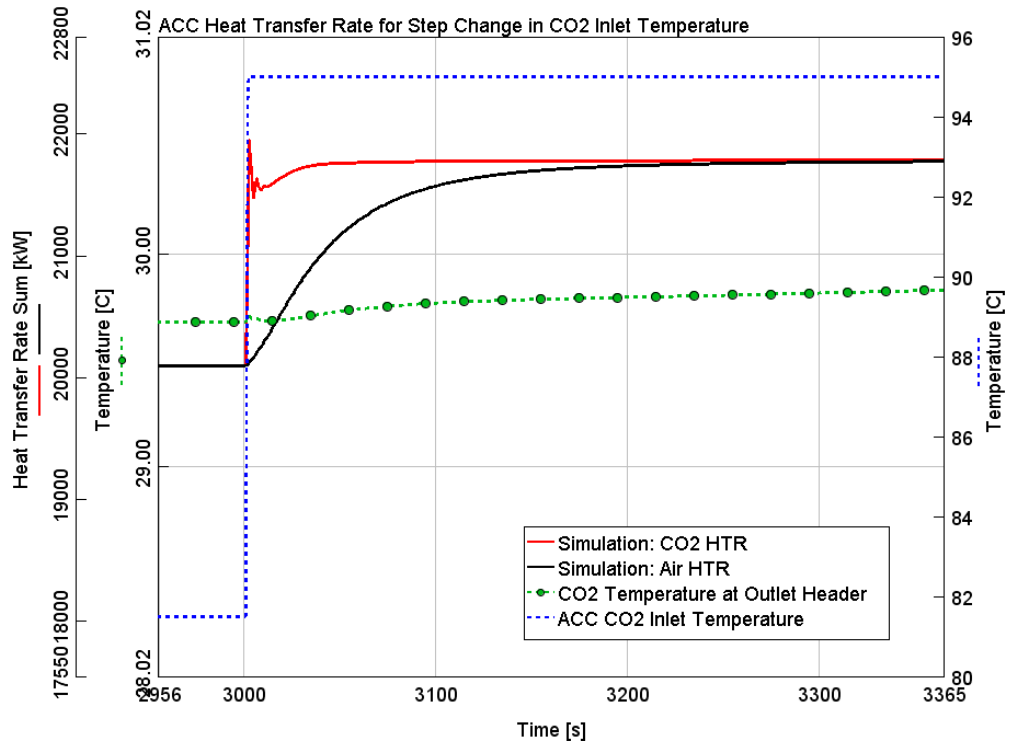


Figure 21: ACC transient response for a step change in CO₂ inlet temperature